Hypotheses for Near-Surface Exchange of Methane on Mars

Renyu Hu,[1,2] A. Anthony Bloom,[1] Peter Gao,[2] Charles E. Miller,[1] and Yuk L. Yung[1,2]

Abstract

The Curiosity rover recently detected a background of 0.7 ppb and spikes of 7 ppb of methane on Mars. This *in situ* measurement reorients our understanding of the martian environment and its potential for life, as the current theories do not entail any geological source or sink of methane that varies sub-annually. In particular, the 10-fold elevation during the southern winter indicates episodic sources of methane that are yet to be discovered. Here we suggest a near-surface reservoir could explain this variability. Using the temperature and humidity measurements from the rover, we find that perchlorate salts in the regolith deliquesce to form liquid solutions, and deliquescence progresses to deeper subsurface in the season of the methane spikes. We therefore formulate the following three testable hypotheses. The first scenario is that the regolith in Gale Crater adsorbs methane when dry and releases this methane to the atmosphere upon deliquescence. The adsorption energy needs to be 36 kJ mol^{-1} to explain the magnitude of the methane spikes, higher than existing laboratory measurements. The second scenario is that microorganisms convert organic matter in the soil to methane when they are in liquid solutions. This scenario does not require regolith adsorption but entails extant life on Mars. The third scenario is that deep subsurface aquifers produce the bursts of methane. Continued *in situ* measurements of methane and water, as well as laboratory studies of adsorption and deliquescence, will test these hypotheses and inform the existence of the near-surface reservoir and its exchange with the atmosphere. Key Words: Mars—Methane—Astrobiology—Regolith. Astrobiology 16, 539–550.

1. Introduction

METHANE (CH$_4$) is an organic molecule in Earth's atmosphere primarily produced by living organisms (Seinfeld and Pandis, 2006). It has also been measured in Mars' atmosphere by telescopic and spacecraft remote sensing (Formisano *et al.*, 2004; Krasnopolsky *et al.*, 2004; Mumma *et al.*, 2009). However, these measurements produced inconsistent results, and some of these measurements have been called into question (*e.g.*, Zahnle *et al.*, 2011). Recently, an *in situ* measurement of methane on Mars has been made: Mars Science Laboratory's (MSL's) Tunable Laser Spectrometer (TLS) as a part of the Sample Analysis at Mars (SAM) instrument determined a background CH$_4$ mixing ratio of ∼0.7 ppbv and a pulse of ∼7 ppbv observed over 2 months (Webster *et al.*, 2015). These measurements suggest strong temporal variability of the methane abundance on the surface of Mars.

Methane's atmospheric existence requires a geologically recent or continually replenishing source, because methane has a lifetime of ∼300 years in Mars' oxidizing atmosphere (Nair *et al.*, 1994; Summers *et al.*, 2002). This source can be photodegradation of organic matter in the meteorites fallen onto Mars (Keppler *et al.*, 2012; Moores and Schuerger, 2012; Schuerger *et al.*, 2012). Alternatively, methane has to come from Mars itself, which challenges the conventional understanding of a geologically and biologically dead Mars (*e.g.*, Lyons *et al.*, 2005; Atreya *et al.*, 2007). An indigenous source of methane is corroborated by a recent discovery of methane evolved from martian meteorites (Blamey *et al.*, 2015). Furthermore, atmospheric processes alone cannot produce the variability of methane detected by Curiosity, because the atmospheric mixing time of methane is much shorter than its chemical lifetime (Lefèvre and Forget, 2009). The discovery of methane thus compels a new chapter of Mars research to explain the existence of methane and its variability in the martian atmosphere.

Extrapolating our knowledge of terrestrial biotic sources to Mars, many consider methanogens (a type of CH$_4$-producing archaean microbe) as a probable analogue to martian life-forms (Boston *et al.*, 1992; Weiss *et al.*, 2000; Schulze-Makuch *et al.*, 2008). Some methanogens are able

to utilize inorganic compounds (H_2 and CO_2) as their only source of energy and produce methane. Being independent of photosynthesis for subsistence, methanogens can thrive in the deep subsurface where CO_2 is the predominant oxidant and H_2(aq) is abundant from water-rock interactions [e.g., ferrous-iron reduction of H_2O to H_2 during serpentinization (Lyons et al., 2005; Chassefière and Leblanc, 2011)]. H_2 may also come from photolysis of H_2O in the atmosphere (Weiss et al., 2000). In fact, methanogens thrive in some of the harshest environments on Earth, including extremely acidic environments and inside Greenland glacial ice 3 km deep, which is analogous to martian subsurface ice environments (Stevens and McKinley, 1995; Chapelle et al., 2002; Tung et al., 2005; Walker et al., 2005).

Alternatively, Fischer-Tropsch-type (FTT) reactions can be a potential methane source (Oze and Sharma, 2005; Atreya et al., 2007; Etiope and Sherwood Lollar, 2013). FTT production is the most widely posited abiotic source of methane on Earth. Catalyzed by transition metals and related oxides, these reactions have the same overall chemistry as the methanogenesis, take place in hydrothermal environments, and probably source H_2 also from serpentinization. Abundant evidence indicates that volcanism and hydrothermal environments existed, and might still exist, on Mars (Schulze-Makuch et al., 2008; Squyres et al., 2008; Hauber et al., 2011). These environments provide heat and liquid water to support FTT and/or microbial CH_4 production. Thus, atmospheric CH_4 may point to either serpentinization or the existence of life itself, both of which are associated with a warm, habitable backdrop.

In this paper, we focus on the singularly important discovery of the episodically enhanced CH_4 emission on Mars. The elevated methane levels occurred in the southern-hemisphere winter, except for a single and statistically marginal measurement on Sol 306 (Webster et al., 2015).

A first-order question about Curiosity's methane spikes is whether they represent a new source to the atmosphere or some cyclic processes that conserve methane. If the methane spikes represent new methane produced from the deep subsurface (Atreya et al., 2007) or from a meteoritic source (Fries et al., 2015), then this methane would be oxidized and remain in the martian atmosphere in the form of CO_2. As a lower estimate, if 7 ppb of methane is produced per year across the entire martian surface (representing the spike from $L_s \sim 50°$ to 90°), then over 3 billion years, the total amount of CO_2 produced is 20 times the present atmospheric CO_2 content. This is much higher than the Amazonian outgassing rates determined from photogeological constraints (Greeley and Schneid, 1991; Grott et al., 2011) or what would be allowed by atmospheric evolution models (Chassefière and Leblanc, 2011; Hu et al., 2015). On the other hand, if the methane is converted to organics and stored in the regolith, then the molar density of organics originating from methane would be (8.4/d) moles per gram of soil, assuming C_6H_5Cl as the organic molecule, with d as the depth in the soil in units of centimeters to which the organics are stored. This is far greater than the observed molar density for any reasonable values of d (Freissinet et al., 2015). Therefore, if the spikes are new methane, the source must be local; alternatively, the spikes are signatures of cyclic processes that produce fast source and sink.

Interestingly, the methane spikes were coincident with surface relative humidities greater than 60% measured by the Rover Environmental Monitoring Station (REMS) (Webster et al., 2015). This apparent correlation motivates us to consider the surface-atmosphere exchange as a major modulator for the atmospheric methane abundances in Gale Crater, the landing site of MSL.

A high surface relative humidity may have a strong impact on the atmosphere-surface exchange because perchlorate salts in the regolith may deliquesce to form liquid solutions (Martín-Torres et al., 2015). Martian regolith contains $\sim 0.5\%$ perchlorate salts by weight, measured at both the Phoenix and the Curiosity landing sites (Hecht et al., 2009; Leshin et al., 2013; Ming et al., 2014). They can form liquid solutions under martian conditions due to their low eutectic temperatures and low deliquescence relative humidities (DRHs) (Marion et al., 2010; Martínez and Rennó, 2013; Fischer et al., 2014; Nuding et al., 2014; Toner et al., 2014; Martín-Torres et al., 2015). Recent laboratory measurements have determined that the DRH of calcium perchlorate is only $\sim 50\%$ at 198 K and that the wet salt does not lose moisture until the relative humidity drops to $\sim 15\%$ (Nuding et al., 2014). By comparing the eutectic temperature and the DRH to the measured surface temperature and relative humidity, we confirm that perchlorate salts in the subsurface of Gale Crater may deliquesce in the southern winter, in which the methane spikes were measured.

We therefore formulate three hypotheses in an attempt to explain the variability of the atmospheric methane abundance at Gale Crater. The first hypothesis (Hypothesis I) is that the regolith in Gale Crater adsorbs methane when dry and releases this methane to the atmosphere when the relative humidity in the regolith is high enough for perchlorate salts to deliquesce. The second hypothesis (Hypothesis II) is that microorganisms convert organic matter in the soil to methane when they are in liquid solutions. This scenario does not require regolith adsorption. The third hypothesis (Hypothesis III) is that deep subsurface aquifers produce the bursts of methane. The first two hypotheses explain the methane spikes as signatures of cyclic processes that produce fast source and sink, whereas the third hypothesis explains the methane spikes as local emission of new methane.

2. Subsurface Temperature and Humidity Models

We model the subsurface temperature and humidity of dusty terrains at Gale Crater by solving diffusion equations of heat and moisture with the hourly averaged REMS data as the boundary conditions (Gómez-Elvira et al., 2012). The absolute humidity of each measurement is computed from the measured relative humidity and the sensor temperature archived in NASA's Planetary Data System (https://pds.nasa.gov), with the saturation vapor pressure from Murphy and Koop (2005). The uncertainty of each surface temperature measurement is ~ 5 K at low temperatures (Gómez-Elvira et al., 2014), and the uncertainty of each relative humidity measurement is <2% (Harri et al., 2014). The combined uncertainty of the hourly averaged values is 1 order of magnitude smaller for Gaussian statistics. The data clearly shows the effect of the rover traversing diverse terrains, as the magnitudes of the diurnal variations in both temperature and humidity change significantly (Gómez-Elvira et al., 2014; Harri et al., 2014). To remove this effect, we use daily means for a martian year (from Sol 39 to Sol 707) and add the hourly means from Sol 70 to Sol 89 (when the rover is at Rocknest, a

dusty terrain) to the daily means. We use the diurnal variation measured over a dusty terrain as a proxy for regolith diurnal temperature and moisture variability. We neglect the seasonal change in the magnitude of the diurnal variation in temperature and humidity, which is valid given the equatorial location of Gale Crater.

The REMS relative humidity data in the daytime are thought to be unreliable, because the daytime relative humidity is often lower than 2% (Harri *et al.*, 2014). Multiplied by the saturation vapor concentration, the REMS daytime relative humidity measurements imply atmospheric water concentrations up to 3×10^{-5} kg m^{-3}. This water concentration appears to be too large compared with the column water abundances in the equatorial region. The Mini-TES instrument on Spirit and Opportunity rovers measured daytime water columns seasonally variable from a few to 20 pr. μm (Smith *et al.*, 2006). The TES instrument on board Mars Global Surveyor also indicated a peak daytime water column of 20 pr. μm (Smith, 2004). Using a boundary layer thickness of 5 km (Savijarvi *et al.*, 2015), this column corresponds to a concentration of 4×10^{-6} kg m^{-3} at the surface. If the boundary layer has a thickness of 2 km, the surface concentration can be up to 1×10^{-5} kg m^{-3}. However, what if the REMS daytime data are actually right? A detailed inspection reveals that the several hundred measurements in each hour in the daytime are not consistent with a random noise around zero. The standard deviation of each group of measurements is small enough to statistically declare a nonzero mean value at 10 - σ or higher. Of course, the standard deviation may be artificially small as a result of the data processing pipeline. We therefore consider all these possibilities of daytime water concentration in the analysis: for Case L (low water concentration) we impose an upper limit of 4×10^{-6} kg m^{-3} on the REMS data; for Case M (intermediate water concentration) we impose an upper limit of 1×10^{-5} kg m^{-3}; and for Case H (high water concentration) we use the REMS data as reported in the Planetary Data System.

The thermal and moisture diffusion equations are solved on a 41-level grid from zero to 5.2 m (*i.e.*, four thermal skin depths). The size of layers increases with depth, and the smallest size is 0.01 cm at the shallow subsurface. We use the thermal inertia derived for Rocknest (Martínez *et al.*, 2014) and the volumetric heat capacity for the martian eolian dunes (Edgett and Christensen, 1991). Figure 1 shows the modeled subsurface temperature. The moisture diffusion equation [*i.e.*, Eq. 13 in Zent *et al.* (1993)] includes physical adsorption and desorption by regolith, condensation, and corrections due to soil porosity and tortuosity (Mellon and Jakosky, 1993; Zent *et al.*, 1993). We assume a soil porosity of 0.5 and a porosity/tortuosity ratio of 0.3 (Sizemore and Mellon, 2008). Physical adsorption and desorption is assumed to be in equilibrium and follows a Langmuir-Freundlich isotherm measured for palagonite, a terrestrial analogue of martian basaltic soil (Zent and Quinn, 1997). The effect of physical adsorption and desorption is to retard water vapor diffusion by several orders of magnitude (Fanale and Cannon, 1971; Zent and Quinn, 1997). Figure 2 shows the modeled subsurface relative humidity for three assumptions of the daytime water concentration.

The diurnal variation of relative humidity extends to a depth of ~ 10 cm, on the same order of magnitude as the diurnal temperature variation. Below the depth of diurnal

variation, the relative humidity is constantly below 20%, except for the southern winter, during which the relative humidity can be as high as 50% within the depth of 1 m for the high water concentration scenario (Fig. 2). Further inspection of the results reveals that the absolute humidity below the depth of diurnal variation actually has little seasonal variation, consistent with the picture that water vapor diffusion is significantly retarded by physical adsorption. Therefore, the seasonally high subsurface relative humidity is driven by the seasonally low subsurface temperature as shown in Fig. 1. Furthermore, a zoom-in view of the relative humidity variation indicates that condensation can occur near the surface early morning during the southern winter (Fig. 2), a finding consistent with that of Martín-Torres *et al.* (2015).

The modeled temperature and relative humidity are then compared with the experimentally measured DRH for perchlorate (Nuding *et al.*, 2014) to determine whether deliquescence occurs (Fig. 3). We assume calcium perchlorate because both Phoenix and Curiosity identify calcium perchlorate as the likely form of the parent salt (Glavin *et al.*, 2013; Kounaves *et al.*, 2014). We find that the surface temperature and humidity conditions allow deliquescence to occur in the top 5–15 cm of soil, each sol before sunrise and after sunset (Fig. 3). The liquid solution does not persist over diurnal cycles close to the surface. The depth range of the transient liquid solution varies with the surface daily mean temperature and is largest in the southern winter.

For a conservative daytime water concentration of 4×10^{-6} kg m^{-3} or lower (Case L), deliquescence only occurs in the shallow subsurface and results in transient solutions. This is consistent with the findings of Martín-Torres *et al.* (2015), in which they omitted all daytime relative humidity measurements. Nonetheless, if the daytime water concentration is indeed higher, our calculation indicates that persisting liquid solutions could occur below the shallow subsurface in the southern winter, starting from $L_S \sim 50°$[1] (Fig. 3, Cases M and H). The range of the liquid solution is larger for a higher water concentration. Because of a small diffusion coefficient, the absolute humidity of the soil at depths is roughly constant. The deep liquid solution is formed by slow cooling of the deep soil and the increase of the relative humidity. The liquid solution persists to $L_S \sim 180$–210°, longer than the high relative humidity season, manifesting hysteresis.

3. Hypothesis I: Deliquescence-Modulated Adsorption and Desorption of Methane

This scenario assumes that methane is normally adsorbed by the regolith. However, when deliquescence occurs, the liquid solutions of perchlorate that form can conceivably coat the soil particles and deactivate most active sites, releasing methane into the atmosphere. Wetted particles have much smaller surface area than dry particles. Ten-micrometer round-shaped particles of basaltic composition only have a surface area of ~ 0.15 m^2 g^{-1}, and this is even smaller for larger particles. Dry regolith on Mars, however, has a surface area ~ 17–100 m^2 g^{-1} (Ballou and Wood, 1978; Zent and

---

[1]The solar longitude L_S is the Mars-Sun angle, measured from the northern-hemisphere spring equinox where $L_S = 0$. For the southern hemisphere, $L_S = 90$ corresponds to winter solstice, and $L_S = 270$ corresponds to summer solstice.
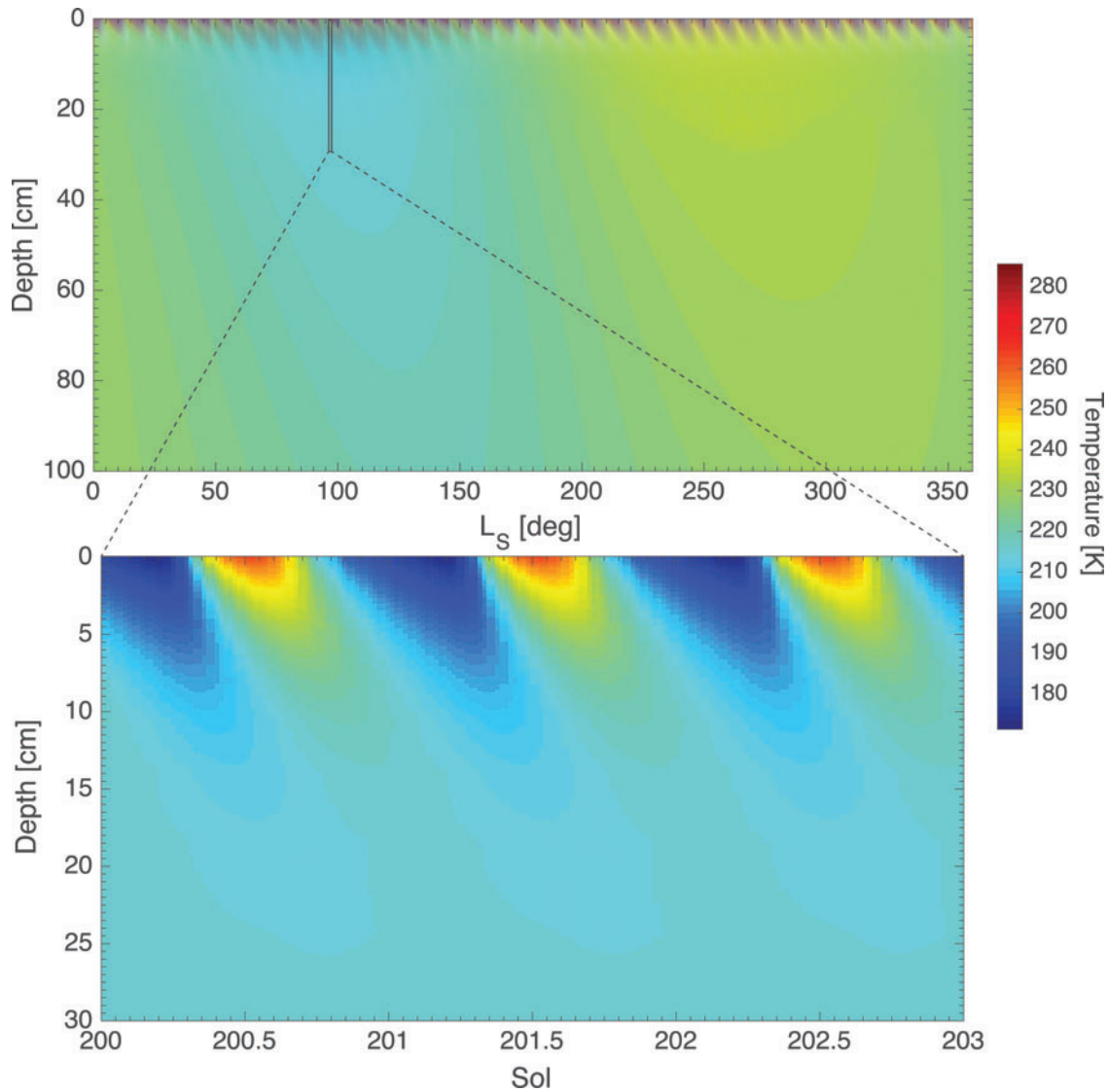
FIG. 1. Subsurface temperature derived from REMS surface temperature measurements. The bottom panel provides a zoom-in view of the top panel over 3 sols. Diurnal temperature variation is limited to a depth of a few centimeters, and seasonal temperature variation extends to ~ 1 m. (Color graphics available at www.liebertonline.com/ast)

Quinn, 1997; Meslin *et al.*, 2011). It is therefore plausible to hypothesize that wetting could effectively remove surface area and displace adsorbed methane. The methane is then mixed in the planetary boundary layer and may be transported and re-adsorbed by the regolith elsewhere.

Taking the boundary layer as a box (*e.g.*, 33% of the column mass for a boundary layer thickness of 5 km), the column mass of methane in the box (M_{CH4}) is modeled by the following equation,

$$\frac{dM_{CH_4}}{dt} = F_{Background} - \frac{M_{CH_4}}{t_{res}} + F_{Deliquescence} \quad (1)$$

t_{res} is the local atmospheric residence time of methane that brackets removal of methane by diurnal thermal tides, horizontal advection and diffusion, and soil adsorption. The horizontal advection and diffusion can be a sink in this model because Gale Crater is not fully covered with thick regolith,

so spreading methane emitted from regions of thick regolith across Gale Crater can greatly reduce the local methane concentration. t_{res} is taken as a free parameter, because the footprint of the methane emission is unknown. $F_{Background}$ is the flux of methane to maintain the 0.7 ppb background level of methane, and is equal to $(M_{CH_4})_{Background}/t_{res}$. $F_{Background}$ is invoked to complete the equation, and it represents the partitioning of methane between the atmosphere and the regolith. Equation 1 can be rewritten using the departure from the background level M_{CH_4} - $(M_{CH_4})_{Background}$ as the variable and without the $F_{Background}$ term.

Once deliquescence occurs, the displaced methane is assumed to be released to the atmosphere immediately. This is probably close enough to reality because the deliquescence starts from the shallow subsurface and progresses deeper, because solubility of methane in salty water is negligible, and because the diffusivity of methane is fast enough such that it should quickly reach the surface
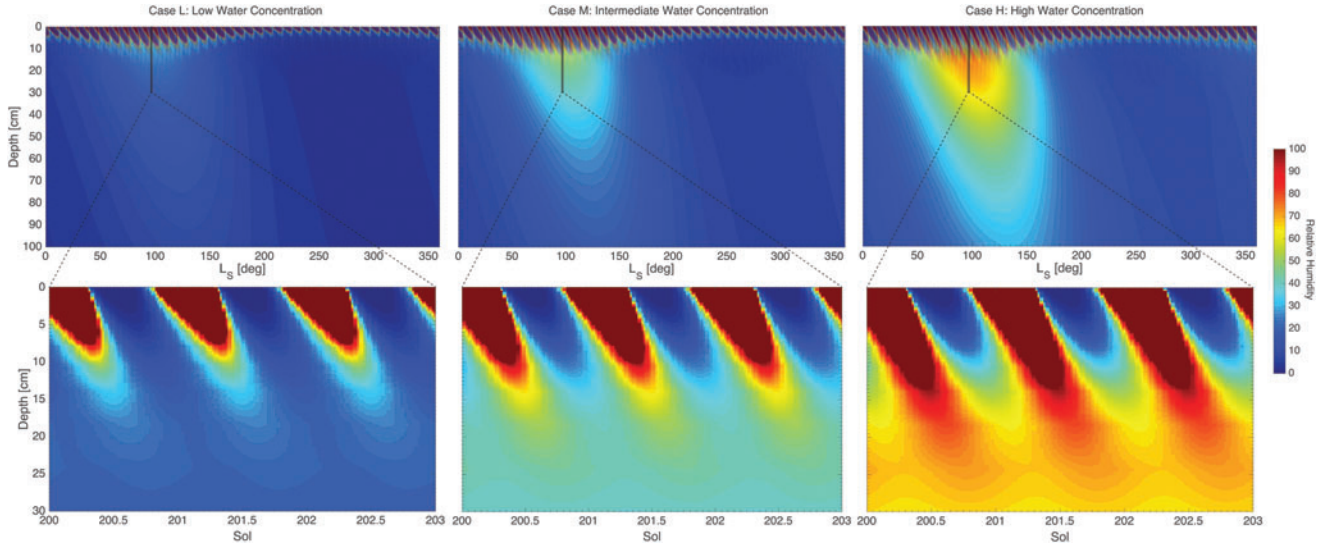
FIG. 2. Subsurface relative humidity derived from REMS surface temperature and near-surface relative humidity measurements. The bottom panels provide zoom-in views of the top panels over 3 sols. The three columns correspond to three cases for daytime water concentration. (Color graphics available at www.liebertonline.com/ast)

(Gough *et al.*, 2010). The flux of methane produced by the onset of deliquescence is

$$F_{\text{Deliquescence}} = \frac{d}{dt}\int_{\text{Deliquescence}} \rho_s \gamma_{CH_4} m_{CH_4} A_s \theta_{CH_4} dz \quad (2)$$

where $\rho_s \sim 1300 \, \text{kg} \, \text{m}^{-3}$ is soil density, $\gamma_{CH_4} = 5.2 \times 10^{18} \, \text{m}^{-2}$ is the monolayer coverage of methane per unit surface area (Gough *et al.*, 2010), m_{CH_4} is the mass of methane molecule, θ_{CH_4} is the coverage ratio of the methane, and $A_s \sim 17$–$100 \, \text{m}^2 \, \text{g}^{-1}$ is the specific surface area. The specific surface area adopted in the study is estimated based on *in situ* measurements of Viking (Ballou and Wood, 1978) or measurements of JSC Mars-1 analogue (Meslin *et al.*, 2011). The specific surface area could be as high as $1000 \, \text{m}^2 \, \text{g}^{-1}$ if the soil was mainly made of clay minerals (Zent and Quinn, 1997), which is not seen in Gale Crater.

θ_{CH_4} is calculated from the Langmuir isotherm,

$$\theta_{CH_4} = \frac{K_{eq} n_{CH_4}}{1 + K_{eq} n_{CH_4} + K'_{eq} n_{CO_2}} \quad (3)$$

where n_{CH_4} is the number density of methane in the gas phase, and

$$K_{eq} = \frac{vh}{4\gamma_{CH_4} + k_b T} \exp(E_a/RT) \quad (4)$$

where v is the thermal velocity of methane, h is Planck's constant, k_b is the Boltzmann constant, R is the gas constant, and E_a is the adsorption energy. n_{CO_2} is the number density of CO_2, and K'_{eq} is the equilibrium constant for CO_2 adsorption. Equation 3 is applicable with CO_2 being the sole competing substance for adsorption, because CO_2 ice cannot form in Gale Crater, H_2O ice may form but only at the top $5 \sim 10 \, \text{cm}$ of soil during nighttime, and inhomogeneous grains, like perchlorate grains, only make less than 1% of soil mass. Given that in any case $K_{eq} n_{CH_4} \ll 1$, Eq. 3 is reduced to

$$\theta_{CH_4} = K_{eq} n_{CH_4} (1 - \theta_{CO_2}) \quad (5)$$

where θ_{CO_2} is the coverage ratio of CO_2,

$$\theta_{CO_2} = \frac{K'_{eq} n_{CO_2}}{1 + K'_{eq} n_{CO_2}} \quad (6)$$

We adopt the θ_{CO_2} measurement for palagonite under martian conditions fitted to the format of Eq. 6 by Zent and Quinn (1995).

E_a has been measured over the martian soil analogue JSC Mars-1, and the measured value is $18 \pm 2 \, \text{kJ} \, \text{mol}^{-1}$ (Gough *et al.*, 2010). We, however, postulate that the detail surface properties could matter for the amount of methane adsorption, specified by E_a in our formulation. To account for model uncertainties, including surface properties, advection, diffusion, and the effect of topography on diurnal CH_4 accumulation, we treat E_a and t_{res} as free parameters.

We solve Eqs. 1–2 to determine whether methane adsorption and desorption would contribute to the variability seen in Gale Crater. Figure 4 shows the best-fit models for Case L (low water concentration) and Case H (high water concentration). We only include the day-to-day change in the range of deliquescence when evaluating Eq. 2. This is because adsorption of methane is kinetically slow (Gough *et al.*, 2010) and a diurnal deliquescence-efflorescence cycle would not allow the soil to be loaded by methane when dry. We hypothesize that the seasonal variation in the maximum depth of deliquescent soil (Fig. 3) could be the main driver of methane variability in the atmosphere.

Figure 4 shows that deliquescence-induced desorption of methane can account for the methane spikes. The season in which deliquescence progresses to deeper subsurface, in
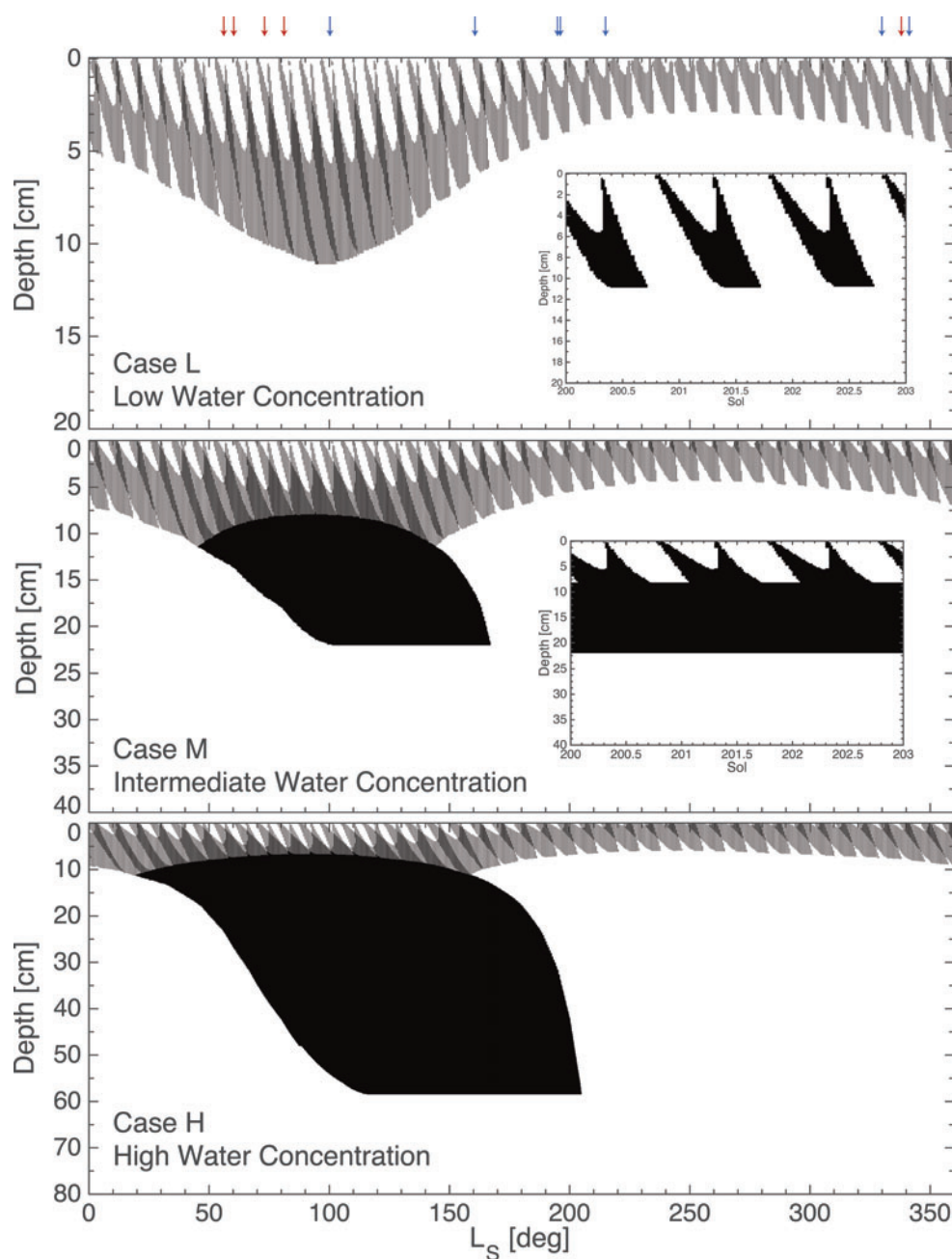
FIG. 3. Subsurface layers in which deliquescent perchlorate solution is expected. The depth range in which calcium perchlorate salts are deliquescent and forming liquid brine is shown in black. The three panels correspond to three cases for daytime water concentration. Note different vertical scales among the panels. The two inserts provide zoom-in views of 3 sols to illustrate the diurnal cycle of deliquescence and efflorescence in the shallow subsurface. The arrows on the top indicate the L_S when SAM's methane measurements were taken, with the blue arrows indicating background measurements and the red arrows indicating the spike measurements. (Color graphics available at www.liebertonline.com/ast)

both low and high water cases, is consistent with the season in which the methane spikes are measured (*i.e.*, the beginning of southern winter). The methane released from the regolith can quickly dissipate, consistent with the rapid drop-off at $L_S \sim 100°$, for a residence time of a few days. A small residence time indicates a small footprint of the methane source in Gale Crater and fast re-adsorption of methane to the regolith. This model does not predict a methane spike at $L_S \sim 330°$. However, given the low sig-

nificance of the measurement, the overall goodness of fit achieved by this hypothesis ($\chi^2/dof \sim 1.4$) is satisfactory.

The main challenge of this model is that the adsorption energy required is 2-fold greater than what is measured by Gough *et al.* (2010). This is because a sufficient amount of methane needs to be temporarily stored in the upper 10 cm (Case L) or 60 cm (Case H) of the soil layer to account for the 7 ppb spike. Increasing the residence time (*e.g.*, en-larging the footprint) could help reduce the adsorption
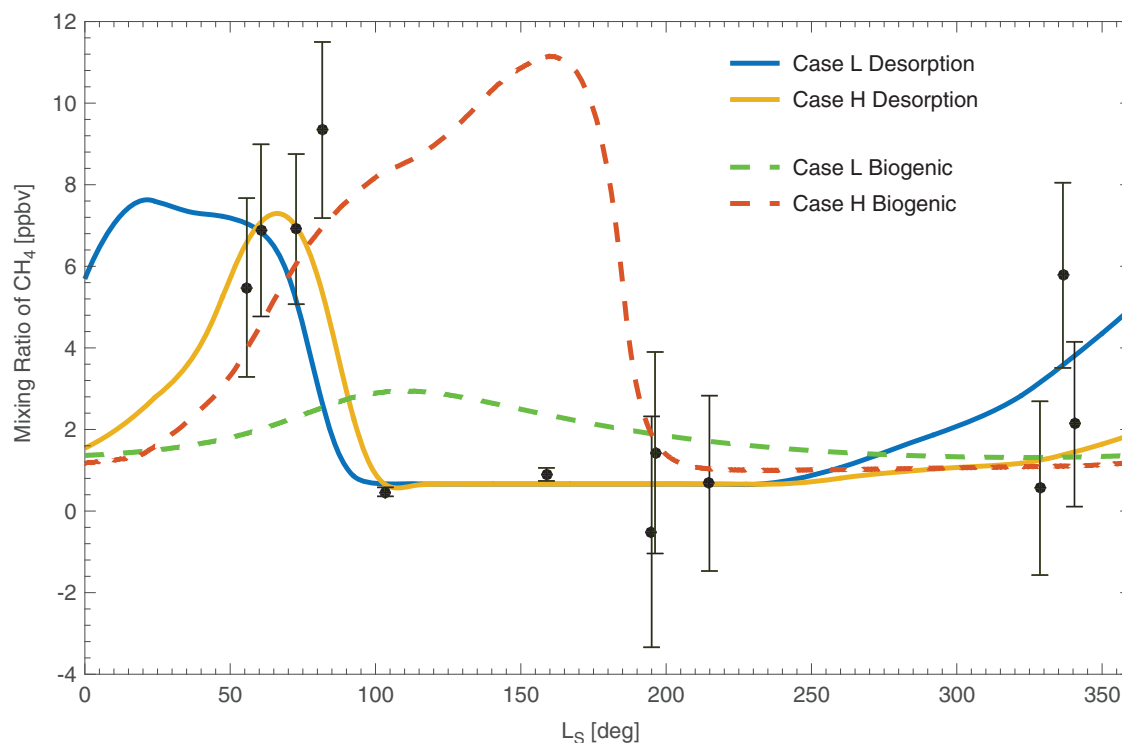
FIG. 4. Models of methane variability due to deliquescence-induced adsorption and desorption (Hypothesis I) or deliquescence-enabled methanogenesis (Hypothesis II) in comparison with MSL measurements (Webster *et al.*, 2015). For Hypothesis I, the best-fit model of Case L (low water concentration) requires an adsorption energy of 37.2 kJ mol^{-1} and a residence time of 12 days. The goodness of fit is $\chi^2/dof = 2.2$. The best-fit model of Case H (high water concentration) requires an adsorption energy of 36.4 kJ mol^{-1} and a residence time of 4 days. The goodness of fit is $\chi^2/dof = 1.4$. For Hypothesis II, none of the models produce a good fit because of the high flux at $L_S \sim 100°$. We instead show two examples for illustration: both cases assume a baseline residence time of soil carbon of 30 days; Case L assumes t_{res} of 100 sols, and Case H assumes t_{res} of 10 sols. (Color graphics available at www.liebertonline.com/ast)

energy, but the residence time is limited by the firm non-detection at $L_S \sim 100°$. How is the required adsorption energy compared with that of methane for other materials? Existing measurements, often performed under room or higher temperatures, suggest a fairly wide range of adsorption energy: 15–25 kJ mol^{-1} for various kinds of zeolites (Zhang *et al.*, 1991; Cavenati *et al.*, 2004; Himeno *et al.*, 2007), 16–21 kJ mol^{-1} for activated carbons (Himeno *et al.*, 2005), and 39 kJ mol^{-1} for a synthetic nanoporous titanium silicate (Delgado *et al.*, 2008). Further laboratory studies are warranted to determine whether the high adsorption energy required by this scenario is possible for martian regolith.

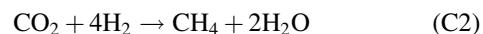## 4. Hypothesis II: Biological Conversion between Organic Matter and Methane

This scenario postulates extant microorganisms in the regolith and assumes that in the presence of liquid water and organic compounds these microorganisms are able to produce methane. Like Hypothesis I, this hypothesis is based on the seasonal deliquescence-efflorescence cycle, but it does not require a large adsorption energy.

This hypothesis is motivated by the recent discovery of organic matter in drill samples of a mudstone in the Yellowknife Bay region of Gale Crater (Freissinet *et al.*, 2015). The detected organic matter includes trace-level chlorobenzene (C_6H_5Cl) and dichloroalkanes ($C_3H_6Cl_2$) in the evolved gases, whose precursors are suggested to be ben-

zenecarboxylates and aliphatic hydrocarbons. Benzene rings are hard to break, but one may imagine microorganisms instead use the aliphatic hydrocarbons by performing the following hydrogenation reaction

$$C_3H_8 + 2H_2 \rightarrow 3CH_4 \tag{C1}$$

which is exothermic ($\Delta_r G° = -129.0$ kJ mol^{-1}). Alternatively, methanogens could directly source carbon from the atmosphere

$$CO_2 + 4H_2 \rightarrow CH_4 + 2H_2O \tag{C2}$$

The source of hydrogen for this metabolism is photochemical dissociation of water vapor in the atmosphere (Weiss *et al.*, 2000). We imagine yeastlike microorganisms performing the biochemical reactions above in liquid solutions formed by deliquescence of perchlorate salts.

On Earth, methanogenesis occurs as a result of oxygen-depleted decomposition of organic C compounds, and methanogens consume acetate (CH_3COOH) to produce CH_4 and CO_2, or CO_2 and H_2 to produce CH_4 and H_2O (Whalen, 2005). The present-day production of CH_4 predominantly occurs in water-logged, oxygen-depleted (anaerobic) environments. Temperature is a limiting factor to methanogenesis: CH_4 emissions from soils have been found to vary exponentially as a function of temperature (Van Hulzen *et al.*, 1999; Bloom *et al.*, 2010; Yvon-Durocher *et al.*, 2014). Other factors

that influence the production of CH_4 in oxygen-depleted environments include soil pH and redox potential (Bloom *et al.*, 2012).

Life is known to exist in highly salty and highly saline environments on Earth (Boetius and Joye, 2009; Stueken *et al.*, 2015). However, it is doubtful that any terrestrial microorganisms, even those living in highly saline environments, can live in a eutectic brine of Ca perchlorate on Mars, because the water activity on Mars would be too low (Rummel *et al.*, 2014). Phenomenologically, and as a bold assumption, we consider the possibility that martian life has developed a biological mechanism that allows functioning in such a harsh environment.

Assuming methanogenesis occurs in Gale Crater, we model

$$\frac{dM_{CH_4}}{dt} = F_{Background} - \frac{M_{CH_4}}{t_{res}} + F_{Methanogen} \quad (7)$$

Here, t_{res} includes not only horizontal transport and physical adsorption but also conversion from methane back to organic matter, probably by methanotrophs (see Fig. 5), given that CH_4 oxidation in aerobic and anaerobic environments is a source of C and energy for terrestrial methanotrophs (Whalen, 2005; Treude *et al.*, 2007). $F_{Methanogen}$ is the methane flux produced by methanogens, which is modeled as

$$F_{Methanogen} = \frac{C\rho_s}{t_0} \int_{Deliquescence} Q_{10}^{\frac{T-273.15}{10}} dz \quad (8)$$

where $C = 5 \times 10^{-8}$ kg kg^{-1} is the soil content of aliphatic hydrocarbons, t_0 is the baseline residence time of organic carbon at 0°C, and Q_{10} is an exponential temperature dependence constant. Equation 8 implies that t_0, together with the temperature and the liquid water availability in the soil, determines the residence time of organic carbon in the soil. The measured and modeled biological residence times of carbon in anaerobic environments span across several orders of magnitude [from 30 days for root exudates to 5×10^5 days for soil carbon (Miyajima *et al.*, 1997; Bridgham *et al.*, 1998; Wania *et al.*, 2010)]. We choose $Q_{10} = 2$, broadly
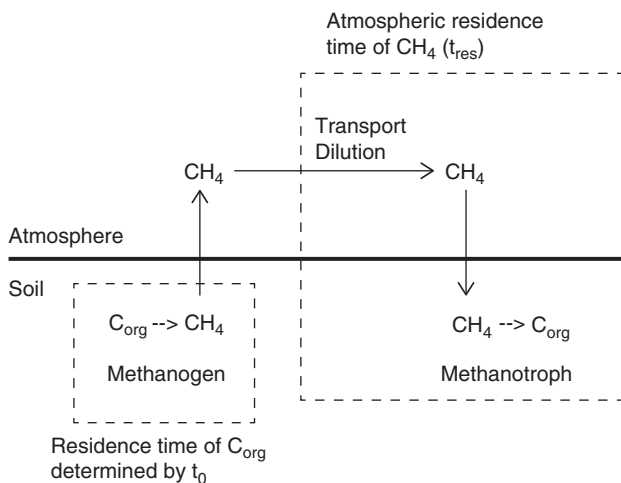
consistent with terrestrial biological methane emission studies (Bloom *et al.*, 2010; Wania *et al.*, 2013; Yvon-Durocher *et al.*, 2014).

The deliquescence-enabled methanogenesis can produce the methane spikes during the southern winter as measured by MSL but cannot produce the rapid drop-off at $L_S \sim 100°$ (Fig. 4). Compared with Hypothesis I, the methane spikes predicted by the methanogenesis model are later in the season. This is simply because the methane emission flux here is proportional to the thickness of the deliquescent soil, while the methane flux due to desorption is proportional to the derivative of that. For the same reason, this hypothesis is not directly consistent with the firm nondetection of elevated methane at $L_S \sim 100°$ or $L_S \sim 150°$, during which the subsurface soil remains wet. It is however possible that MSL was not downstream of the methane source during this period.

A high surface water concentration and then a large thickness of deliquescent soil during winter are probably necessary for methanogenesis to produce the 7 ppb methane spikes. Figure 6 shows the parameter ranges that produce the strength of the spikes. Additionally, one needs to consider replenishment of organic carbon in the soil. The methane production rate is controlled by the baseline residence time of soil carbon (t_0), which is a free parameter in the model. The atmospheric residence time of methane (t_{res}) needs to be shorter than the lifetime of the organic carbon in the soil to ensure replenishment, if the main source of carbon of the methanogens is the soil organic carbon (Reaction C1). In the model we find this condition corresponds to $t_{res} < 20 - 120 \times t_0$, shown as a dashed line in Fig. 6. Using this condition, we find that it is only marginally possible to produce the 7 ppb methane spikes in Case L (low water concentration), while producing the methane spikes in Case H (high water concentration) is much easier. If the methanogens directly source carbon from the CO_2 atmosphere (Reaction C2), the atmospheric residence time of methane can be longer, and the methane spikes are more readily fit by this scenario.
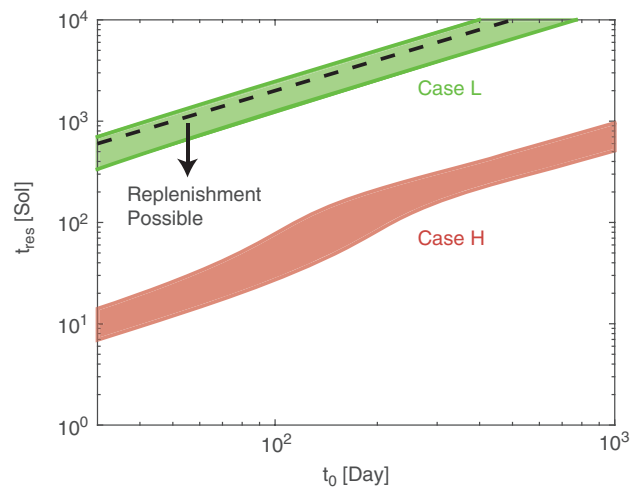

FIG. 5. Schematic illustration of timescales in Hypothesis II: biological conversion between organic matter and methane.

FIG. 6. Parameter ranges for the local atmospheric residence time of methane (t_{res}) and the baseline residence time of soil carbon (t_0) that produce a 7 ± 2 ppb methane spike at $L_S \sim 100°$ as measured by MSL. (Color graphics available at www.liebertonline.com/ast)

5. Hypothesis III: Outbursts from Subsurface Permanent Aquifer

Another possibility is that the elevated methane measured by TLS represents sources of "new" methane emerging from a deep subsurface aquifer. The sources of methane may include subsurface gas-water-rock chemistry and microbial methanogenesis (Lyons *et al.*, 2005; Atreya *et al.*, 2007), with the difference being that biological methanogenesis is much faster than gas-water-rock reactions (Yung *et al.*, 2010). Such a source of methane, along with cometary and meteoric sources, may be necessary to balance the loss of atmospheric methane due to UV photolysis over a timescale of a few hundred years.

A subsurface aquifer may exist at a depth of 5 km assuming a geothermal gradient of $10\,K\,km^{-1}$ (Solomon and Head, 1990; Clifford *et al.*, 2010). The aquifer can be partially sealed by an ice or clathrate layer to produce bursts of methane, in similar ways as the terrestrial arctic tundra. The arctic tundra is one of the major sources of methane for Earth's atmosphere. Concentrated bursts of methane have been observed at tundra sites in late fall as the seasonally thawed active layer refreezes, forcing subsurface methane into the atmosphere (Mastepanov *et al.*, 2008), and during the spring freeze-thaw transition when subsurface methane trapped by the frozen surface escapes (Song *et al.*, 2012). The fall and spring bursts are transitory (occurring only for a <10-day window immediately surrounding the freeze-thaw transition) and episodic (they do not occur every season), and the magnitude of the emissions is highly variable.

On Mars, however, if the methane was released deep from the subsurface, this release should be sporadic and have no seasonality. This is because the seasonal variations of temperature and relative humidity damp out at a depth of a few meters (Fig. 1), and the condition of the permanent aquifer is not controlled by surface conditions. Other geological processes may trigger the subsurface methane to be vented out, such as seepage from mud volcanoes (*e.g.*, Etiope *et al.*, 2011; Komatsu *et al.*, 2011).

The source of methane emission in this scenario must be localized, based on the mass balance calculation in Section 1. A source of methane close to MSL that emits ~7 ppb of methane over a small area could be the cause of the methane spike, while the subsequent decrease back to the background level would be easily explained by the dispersal of the methane into the rest of the atmosphere. The small amount of methane released would have very little effect on the carbon budget of the rest of the atmosphere. It is an open question what areas of Mars would be amenable to such localized methane releases.

6. Conclusion and Prospects

We propose the first working theories that explain the subannual variability of atmospheric methane abundance in Gale Crater, in the form of three testable hypotheses. First, adsorption of methane in the regolith up to a few tens of centimeters' depth, and its release driven by deliquescence during the winter, can explain the apparent methane variability. This scenario requires an adsorption energy 2-fold higher than laboratory measurements on Mars regolith analogues. Second, biological conversion from organic matter to methane in the regolith by microorganisms in perchlorate solutions can produce the magnitude of the methane spikes. However, this model cannot produce the rapid drop-off of the methane

abundance at $L_S \sim 100°$ and likely requires a daytime water concentration higher than standard Mars atmospheric models. Third, the methane spikes may come from a deep subsurface aquifer, representing new methane to the atmosphere. Emitted intermittently, this methane may be the methane that maintains the 0.7 ppb background on a timescale of several hundred years, if the footprint of the emission is small.

Any of the three hypotheses, if confirmed, leads to profound ramifications in our understanding of Mars as an active and potentially habitable world. If adsorption and desorption by regolith modulates atmospheric methane in Gale Crater, greater variability can be expected for higher latitudes, where perchlorate also exists (Hecht *et al.*, 2009) and deliquescence may occur for a larger fraction of the surface (Martínez and Rennó, 2013). The methane variability suggested on the basis of telescopic observations (Mumma *et al.*, 2009), though debated (Zahnle *et al.*, 2011), could be explained in this way. Both the first and the second hypothesis work better when the daytime water concentration at the surface is high. If true, these scenarios warrant further investigation of the boundary layer dynamics and water vapor distribution on Mars. Lastly, if the methane spikes are from the deep subsurface, one might ask how lucky MSL has to be to observe the spikes and whether the geographic low of Gale Crater helps.

Continued monitoring of methane by MSL will test these hypotheses. The first two hypotheses predict the methane variability is seasonal and should repeat annually. The peak of the methane abundance occurs in different seasons between the two hypotheses, with the adsorption-desorption model in the early winter and the methanogenesis model in the later winter. We caution that observing the repeated signals, even if either of the hypotheses is true, can be hard because of the changing wind patterns and the rover location. The last hypothesis predicts the methane spikes are sporadic. Meanwhile, our investigations of the three hypotheses call for laboratory studies of gas adsorption and desorption during deliquescence, as well as further laboratory studies of the adsorption energy of methane for fine, porous silicate materials. Finally, future *in situ* Mars exploration may conduct improved characterization of the daytime water vapor concentration at the surface, and measurement of the water's isotopic signatures will further constrain the rate of the atmosphere-regolith exchange and reveal the smoking gun of a near-surface methane reservoir.

References

Atreya, S.K., Mahaffy, P.R., and Wong, A.-S. (2007) Methane and related trace species on Mars: origin, loss, implications for life, and habitability. *Planet Space Sci* 55:358–369.

Ballou, E.V. and Wood, P.C. (1978) Chemical interpretation of Viking Lander 1 life detection experiment. *Nature* 271:644–645.

Blamey, N.J., Parnell, J., McMahon, S., Mark, D.F., Tomkinson, T., Lee, M., Shivak, J., Izawa, M.R., Banerjee, N.R., and Flemming, R.L. (2015) Evidence for methane in martian meteorites. *Nature Commun* 6, doi:10.1038/ncomms8399.

Bloom, A.A., Palmer, P.I., Fraser, A., Reay, D.S., and Frankenberg, C. (2010) Large-scale controls of methanogenesis inferred from methane and gravity spaceborne data. *Science* 327:322–325.

Bloom, A., Palmer, P., Fraser, A., and Reay, D. (2012) Seasonal variability of tropical wetland CH_4 emissions: the role of the methanogen-available carbon pool. *Biogeosciences* 9:2821–2830.

Boetius, A. and Joye, S. (2009) Thriving in salt. *Science* 324:1523–1525.

Boston, P.J., Ivanov, M.V., and McKay, C.P. (1992) On the possibility of chemosynthetic ecosystems in subsurface habitats on Mars. *Icarus* 95:300–308.

Bridgham, S.D., Updegraff, K., and Pastor, J. (1998) Carbon, nitrogen, and phosphorus mineralization in northern wetlands. *Ecology* 79:1545–1561.

Cavenati, S., Grande, C.A., and Rodrigues, A.E. (2004) Adsorption equilibrium of methane, carbon dioxide, and nitrogen on zeolite 13x at high pressures. *J Chem Eng Data* 49:1095–1101.

Chapelle, F.H., O'Neill, K., Bradley, P.M., Methé, B.A., Ciufo, S.A., Knobel, L.L., and Lovley, D.R. (2002) A hydrogen-based subsurface microbial community dominated by methanogens. *Nature* 415:312–315.

Chassefière, E. and Leblanc, F. (2011) Constraining methane release due to serpentinization by the observed D/H ratio on Mars. *Earth Planet Sci Lett* 310:262–271.

Clifford, S.M., Lasue, J., Heggy, E., Boisson, J., McGovern, P., and Max, M.D. (2010) Depth of the martian cryosphere: revised estimates and implications for the existence and detection of subpermafrost groundwater. *J Geophys Res: Planets* 115, doi:10.1029/2009JE003462.

Delgado, J.A., Uguina, M.A., Agueda, V.I., and Garca-Sanz, A. (2008) Adsorption and diffusion parameters of methane and nitrogen on microwave-synthesized ETS-4. *Langmuir* 24:6107–6115.

Edgett, K.S. and Christensen, P.R. (1991) The particle size of martian aeolian dunes. *J Geophys Res: Planets* 96:22765–22776.

Etiope, G. and Sherwood Lollar, B. (2013) Abiotic methane on Earth. *Rev Geophys* 51:276–299.

Etiope, G., Oehler, D., and Allen, C. (2011) Methane emissions from Earth's degassing: implications for Mars. *Planet Space Sci* 59:182–195.

Fanale, F.P. and Cannon, W.A. (1971) Adsorption on the martian regolith. *Nature* 230:502–504.

Fischer, E., Martnez, G.M., Elliott, H.M., and Rennó, N.O. (2014) Experimental evidence for the formation of liquid saline water on Mars. *Geophys Res Lett* 41:4456–4462.

Formisano, V., Atreya, S., Encrenaz, T., Ignatiev, N., and Giuranna, M. (2004) Detection of methane in the atmosphere of Mars. *Science* 306:1758–1761.

Freissinet, C., Glavin, D.P., Mahaffy, P.R., Miller, K.E., Eigenbrode, J.L., Summons, R.E., Brunner, A.E., Buch, A., Szopa, C., Archer, P.D., Franz, H.B., Atreya, S.K., Brinckerhoff, W.B., Cabane, M., Coll, P., Conrad, P.G., Des Marais, D.J., Dworkin, J.P., Fairèn, A.G., François, P., Grotzinger, J.P., Kashyap, S., ten Kate, I.L., Leshin, L.A., Malespin, C.A., Martin, M.G., Martín-Torres, F.J., McAdam, A.C., Ming, D.W., Navarro-González, R., Pavlov, A.A., Prats, B.D., Squyres, S.W., Steele, A., Stern, J.C., Sumner, D.Y., Sutter, B., Zorzano, M.-P., and the MSL Science Team. (2015) Organic molecules in the Sheepbed mudstone, Gale Crater, Mars. *J Geophys Res: Planets* 120:495–514.

Fries, M., Christou, A., Archer, D., Conrad, P., Cooke, W., Eigenbrode, J., ten Kate, I.L., Matney, M., Niles, P., Sykes, M., Steele, A., and Treiman, A. (2015) A meteor shower origin for martian methane [abstract 5286]. *Meteorit Planet Sci* 50(S1), doi:10.1111/maps.12501.

Glavin, D.P., Freissinet, C., Miller, K.E., Eigenbrode, J.L., Brunner, A.E., Buch, A., Sutter, B., Archer, P.D., Atreya, S.K., Brinckerhoff, W.B., Cabane, M., Coll, P., Conrad, P.G., Coscia, D., Dworkin, J.P., Franz, H.B., Grotzinger, J.P., Leshin, L.A., Martin, M.G., McKay, C., Ming, D.W., Navarro-González, R., Pavlov, A., Steele, A., Summons, R.E., Szopa, C., Teinturier, S., and Mahaffy, P.R. (2013) Evidence for perchlorates and the origin of chlorinated hydrocarbons detected by SAM at the Rocknest aeolian deposit in Gale Crater. *J Geophys Res: Planets* 118:1955–1973.

Gómez-Elvira, J., Armiens, C., Castañer, L., Domínguez, M., Genzer, M., Gómez, F., Haberle, R., Harri, A.-M., Jiménez, V., Kahanpää, H., Kowalski, L., Lepinette, A., Martín, J., Martínez-Frías, J., McEwan, I., Mora, L., Moreno, J., Navarro, S., de Pablo, M., Peinado, V., Peña, A., Polkko, J., Ramos, M., Rennó, N., Ricart, J., Richardson, M., Rodríguez-Manfredi, J., Romeral, J., Sebastián, E., Serrano, J., de la Torre Juárez, M., Torres, J., Torrero, F., Urquí, R., Vázquez, L., Velasco, T., Verdasca, J., Zorzano, M.-P., and Martín-Torres, J. (2012) REMS: the environmental sensor suite for the Mars Science Laboratory rover. *Space Sci Rev* 170:583–640.

Gómez-Elvira, J., Armiens, C., Carrasco, I., Genzer, M., Gómez, F., Haberle, R., Hamilton, V.E., Harri, A.-M., Kahanpää, H., Kemppinen, O., Lepinette, A., Martín Soler, J., Martín-Torres, J., Martínez-Fras, J., Mischna, M., Mora, L., Navarro, S., Newman, C., de Pablo, M.A., Peinado, V., Polkko, J., Rafkin, S.C.R., Ramos, M., Rennó, N.O., Richardson, M., Rodríguez-Manfredi, J.A., Romeral Planelló, J.J., Sebastián, E., de la Torre Juárez, M., Torres, J., Urquí, R., Vasavada, A.R., Verdasca, J., and Zorzano, M.-P. (2014) Curiosity's Rover Environmental Monitoring Station: overview of the first 100 sols. *J Geophys Res: Planets* 119:1680–1688.

Gough, R.V., Tolbert, M.A., McKay, C.P., and Toon, O.B. (2010) Methane adsorption on a martian soil analog: an abiogenic explanation for methane variability in the martian atmosphere. *Icarus* 207:165–174.

Greeley, R. and Schneid, B.D. (1991) Magma generation on Mars: amounts, rates, and comparisons with Earth, Moon, and Venus. *Science* 254:996–998.

Grott, M., Morschhauser, A., Breuer, D., and Hauber, E. (2011) Volcanic outgassing of CO_2 and H_2O on Mars. *Earth Planet Sci Lett* 308:391–400.

Harri, A.-M., Genzer, M., Kemppinen, O., Gómez-Elvira, J., Haberle, R., Polkko, J., Savijärvi, H., Rennó, N., Rodriguez-Manfredi, J.A., Schmidt, W., Richardson, M., Siili, T., Paton, M., Torre-Juarez, M.D., Mäkinen, T., Newman, C., Rafkin, S., Mischna, M., Merikallio, S., Haukka, H., Martín-Torres, J., Komu, M., Zorzano, M.-P., Peinado, V., Vazquez, L., and Urqui, R. (2014) Mars Science Laboratory relative humidity observations: initial results. *J Geophys Res: Planets* 119:2132–2147.

Hauber, E., Brož, P., Jagert, F., Jodłowski, P., and Platz, T. (2011) Very recent and wide-spread basaltic volcanism on Mars. *Geophys Res Lett* 38, doi:10.1029/2011GL047310.

Hecht, M.H., Kounaves, S.P., Quinn, R.C., West, S.J., Young, S.M.M., Ming, D.W., Catling, D.C., Clark, B.C., Boynton, W.V., Hoffman, J., DeFlores, L.P., Gospodinova, K., Kapit, J., and Smith,

P.H. (2009) Detection of perchlorate and the soluble chemistry of martian soil at the Phoenix lander site. *Science* 325:64–67.

Himeno, S., Komatsu, T., and Fujita, S. (2005) High-pressure adsorption equilibria of methane and carbon dioxide on several activated carbons. *J Chem Eng Data* 50:369–376.

Himeno, S., Tomita, T., Suzuki, K., and Yoshida, S. (2007) Characterization and selectivity for methane and carbon dioxide adsorption on the all-silica DD3R zeolite. *Microporous Mesoporous Mater* 98:62–69.

Hu, R., Kass, D.M., Ehlmann, B., and Yung, Y.L. (2015) Tracing the fate of carbon and the atmospheric evolution of Mars. *Nature Commun* 6, doi:10.1038/ncomms10003.

Keppler, F., Vigano, I., McLeod, A., Ott, U., Früchtl, M., and Röckmann, T. (2012) Ultraviolet-radiation-induced methane emissions from meteorites and the martian atmosphere. *Nature* 486:93–96.

Komatsu, G., Ori, G.G., Cardinale, M., Dohm, J.M., Baker, V.R., Vaz, D.A., Ishimaru, R., Namiki, N., and Matsui, T. (2011) Roles of methane and carbon dioxide in geological processes on Mars. *Planet Space Sci* 59:169–181.

Kounaves, S.P., Chaniotakis, N.A., Chevrier, V.F., Carrier, B.L., Folds, K.E., Hansen, V.M., McElhoney, K.M., O'Neil, G.D., and Weber, A.W. (2014) Identification of the perchlorate parent salts at the Phoenix Mars landing site and possible implications. *Icarus* 232:226–231.

Krasnopolsky, V.A., Maillard, J.P., and Owen, T.C. (2004) Detection of methane in the martian atmosphere: evidence for life? *Icarus* 172:537–547.

Lefèvre, F. and Forget, F. (2009) Observed variations of methane on Mars unexplained by known atmospheric chemistry and physics. *Nature* 460:720–723.

Leshin, L.A., Mahaffy, P.R., Webster, C.R., Cabane, M., Coll, P., Conrad, P.G., Archer, P.D., Atreya, S.K., Brunner, A.E., Buch, A., Eigenbrode, J.L., Flesch, G.J., Franz, H.B., Freissinet, C., Glavin, D.P., McAdam, A.C., Miller, K.E., Ming, D.W., Morris, R.V., Navarro-González, R., Niles, P.B., Owen, T., Pepin, R.O., Squyres, S., Steele, A., Stern, J.C., Summons, R.E., Sumner, D.Y., Sutter, B., Szopa, C., Teinturier, S., Trainer, M.G., Wray, J.J., Grotzinger, J.P., and the MSL Science Team. (2013) Volatile, isotope, and organic analysis of martian fines with the Mars Curiosity rover. *Science* 341, doi:10.1126/science.1238937.

Lyons, J.R., Manning, C., and Nimmo, F. (2005) Formation of methane on Mars by fluid-rock interaction in the crust. *Geophys Res Lett* 32, doi:10.1029/2004GL022161.

Marion, G., Catling, D., Zahnle, K., and Claire, M. (2010) Modeling aqueous perchlorate chemistries with applications to Mars. *Icarus* 207:675–685.

Martínez, G. and Rennó, N. (2013) Water and brines on Mars: current evidence and implications for MSL. *Space Sci Rev* 175:29–51.

Martínez, G.M., Rennó, N., Fischer, E., Borlina, C.S., Hallet, B., de la Torre Juárez, M., Vasavada, A.R., Ramos, M., Hamilton, V., Gómez-Elvira, J., and Haberle, R.M. (2014) Surface energy budget and thermal inertia at Gale Crater: calculations from ground-based measurements. *J Geophys Res: Planets* 119:1822–1838.

Martín-Torres, F.J., Zorzano, M.-P., Valentín-Serrano, P., Harri, A.-M., Genzer, M., Kemppinen, O., Rivera-Valentin, E.G., Jun, I., Wray, J., Bo Madsen, M., Goetz, W., McEwen, A.S., Hardgrove, C., Rennó, N., Chevrier, V.F., Mischna, M., Navarro-González, R., Martínez-Frías, J., Conrad, P., McConnochie, T., Cockell, C., Berger, G., Vasavada, A.R., Sumner, D., and Vaniman, D. (2015) Transient liquid water and water activity at Gale Crater on Mars. *Nat Geosci* 8:357–361.

Mastepanov, M., Sigsgaard, C., Dlugokencky, E.J., Houweling, S., Ström, L., Tamstorf, M.P., and Christensen, T.R. (2008) Large tundra methane burst during onset of freezing. *Nature* 456:628–630.

Mellon, M.T. and Jakosky, B.M. (1993) Geographic variations in the thermal and diffusive stability of ground ice on Mars. *J Geophys Res: Planets* 98:3345–3364.

Meslin, P.-Y., Gough, R., Lefvre, F., and Forget, F. (2011) Little variability of methane on Mars induced by adsorption in the regolith. *Planet Space Sci* 59:247–258.

Ming, D.W., Archer, P.D., Glavin, D.P., Eigenbrode, J.L., Franz, H.B., Sutter, B., Brunner, A.E., Stern, J.C., Freissinet, C., McAdam, A.C., Mahaffy, P.R., Cabane, M., Coll, P., Campbell, J.L., Atreya, S.K., Niles, P.B., Bell, J.F., Bish, D.L., Brinckerhoff, W.B., Buch, A., Conrad, P.G., Des Marais, D.J., Ehlmann, B.L., Fairèn, A.G., Farley, K., Flesch, G.J., Francois, P., Gellert, R., Grant, J.A., Grotzinger, J.P., Gupta, S., Herkenhoff, K.E., Hurowitz, J.A., Leshin, L.A., Lewis, K.W., McLennan, S.M., Miller, K.E., Moersch, J., Morris, R.V., Navarro-González, R., Pavlov, A.A., Perrett, G.M., Pradler, I., Squyres, S.W., Summons, R.E., Steele, A., Stolper, E.M., Sumner, D.Y., Szopa, C., Teinturier, S., Trainer, M.G., Treiman, A.H., Vaniman, D.T., Vasavada, A.R., Webster, C.R., Wray, J.J., Yingst, R.A., and the MSL Science Team. (2014) Volatile and organic compositions of sedimentary rocks in Yellowknife Bay, Gale Crater, Mars. *Science* 343, doi:10.1126/science.1245267.

Miyajima, T., Wada, E., Hanba, Y.T., and Vijarnsorn, P. (1997) Anaerobic mineralization of indigenous organic matters and methanogenesis in tropical wetland soils. *Geochim Cosmochim Acta* 61:3739–3751.

Moores, J.E. and Schuerger, A.C. (2012) UV degradation of accreted organics on Mars: IDP longevity, surface reservoir of organics, and relevance to the detection of methane in the atmosphere. *J Geophys Res* 117:E08008, doi:10.1029/2012JE004060.

Mumma, M.J., Villanueva, G.L., Novak, R.E., Hewagama, T., Bonev, B.P., DiSanti, M.A., Mandell, A.M., and Smith, M.D. (2009) Strong release of methane on Mars in northern summer 2003. *Science* 323:1041–1045.

Murphy, D.M. and Koop, T. (2005) Review of the vapour pressures of ice and supercooled water for atmospheric applications. *Q J R Meteorol Soc* 131:1539–1565.

Nair, H., Allen, M., Anbar, A.D., Yung, Y.L., and Clancy, R.T. (1994) A photochemical model of the martian atmosphere. *Icarus* 111:124–150.

Nuding, D., Rivera-Valentin, E., Davis, R., Gough, R., Chevrier, V., and Tolbert, M. (2014) Deliquescence and efflorescence of calcium perchlorate: an investigation of stable aqueous solutions relevant to Mars. *Icarus* 243:420–428.

Oze, C. and Sharma, M. (2005) Have olivine, will gas: serpentinization and the abiogenic production of methane on Mars. *Geophys Res Lett* 32, doi:10.1029/2005GL022691.

Rummel, J.D., Beaty, D.W., Jones, M.A., Bakermans, C., Barlow, N.G., Boston, P.J., Chevrier, V.F., Clark, B.C., de Vera, J.-P.P., Gough, R.V., Hallsworth, J.E., Head, J.W., Hipkin, V.J., Kieft, T.L., McEwen, A.S., Mellon, M.T., Mikucki, J.A., Nicholson, W.L., Omelon, C.R., Peterson, R., Roden, E.E., Sherwood Lollar, B., Tanaka, K.L., Viola, D., and Wray, J.J. (2014) A new analysis of Mars ''Special Regions'': findings of the Second MEPAG Special Regions Science Analysis Group (SR-SAG2). *Astrobiology* 14:887–968.

Savijarvi, H.I., Harri, A.-M., and Kemppinen, O. (2015) Mars Science Laboratory diurnal moisture observations and column simulations. *J Geophys Res: Planets* 120, doi:10.1002/2014JE004732.

Schuerger, A.C., Moores, J.E., Clausen, C.A., Barlow, N.G., and Britt, D.T. (2012) Methane from UV-irradiated carbonaceous chondrites under simulated Martian conditions. *J Geophys Res* 117:E08007, doi:10.1029/2011JE004023.

Schulze-Makuch, D., Fairén, A.G., and Davila, A.F. (2008) The case for life on Mars. *International Journal of Astrobiology* 7:117–141.

Seinfeld, J.H. and Pandis, S.N. (2006) *Atmospheric Chemistry and Physics*, 2nd ed., John Wiley & Sons, New York.

Sizemore, H.G. and Mellon, M.T. (2008) Laboratory characterization of the structural properties controlling dynamical gas transport in Mars-analog soils. *Icarus* 197:606–620.

Smith, M.D. (2004) Interannual variability in TES atmospheric observations of Mars during 1999–2003. *Icarus* 167: 148–165.

Smith, M.D., Wolff, M.J., Spanovich, N., Ghosh, A., Banfield, D., Christensen, P.R., Landis, G.A., and Squyres, S.W. (2006) One martian year of atmospheric observations using MER Mini-TES. *J Geophys Res: Planets* 111, doi:10.1029/2006JE002770.

Solomon, S.C. and Head, J.W. (1990) Heterogeneities in the thickness of the elastic lithosphere of Mars: constraints on heat flow and internal dynamics. *J Geophys Res: Solid Earth* 95:11073–11083.

Song, C., Xu, X., Sun, X., Tian, H., Sun, L., Miao, Y., Wang, X., and Guo, Y. (2012) Large methane emission upon spring thaw from natural wetlands in the northern permafrost region. *Environ Res Lett* 7, doi:10.1088/1748-9326/7/3/034009.

Squyres, S.W., Arvidson, R.E., Ruff, S., Gellert, R., Morris, R.V., Ming, D.W., Crumpler, L., Farmer, J.D., Des Marais, D.J., Yen, A., McLennan, S.M., Calvin, W., Bell, J.F., Clark, B.C., Wang, A., McCoy, T.J., Schmidt, M.E., and de Souza, P.A. (2008) Detection of silica-rich deposits on Mars. *Science* 320:1063–1067.

Stevens, T.O. and McKinley, J.P. (1995) Lithoautotrophic microbial ecosystems in deep basalt aquifers. *Science* 270:450–455.

Stueken, E., Buick, R., and Schauer, A. (2015) Nitrogen isotope evidence for alkaline lakes on late Archean continents. *Earth Planet Sci Lett* 411:1–10.

Summers, M.E., Lieb, B.J., Chapman, E., and Yung, Y.L. (2002) Atmospheric biomarkers of subsurface life on Mars. *Geophys Res Lett* 29, doi:10.1029/2002GL015377.

Toner, J., Catling, D., and Light, B. (2014) The formation of supercooled brines, viscous liquids, and low-temperature perchlorate glasses in aqueous solutions relevant to Mars. *Icarus* 233:36–47.

Treude, T., Orphan, V., Knittel, K., Gieseke, A., and Boetius, A. (2007) Consumption of methane and CO_2 by methanotrophic microbial mats from gas seeps of the anoxic black sea. *Appl Environ Microbiol* 73:2271–2283.

Tung, H.C., Bramall, N.E., and Price, P.B. (2005) Microbial origin of excess methane in glacial ice and implications for life on Mars. *Proc Natl Acad Sci USA* 102:18292–18296.

Van Hulzen, J., Segers, R., Van Bodegom, P., and Leffelaar, P. (1999) Temperature effects on soil methane production: an explanation for observed variability. *Soil Biol Biochem* 31: 1919–1929.

Walker, J.J., Spear, J.R., and Pace, N.R. (2005) Geobiology of a microbial endolithic community in the Yellowstone geothermal environment. *Nature* 434:1011–1014.

Wania, R., Ross, I., and Prentice, I. (2010) Implementation and evaluation of a new methane model within a dynamic global vegetation model: LPJ-WHyMe v1. 3.1. *Geoscientific Model Development* 3:565–584.

Wania, R., Melton, J.R., Hodson, E.L., Poulter, B., Ringeval, B., Spahni, R., Bohn, T., Avis, C.A., Chen, G., Eliseev, A.V., Hopcroft, P.O., Riley, W.J., Subin, Z.M., Tian, H., van Bodegom, P.M., Kleinen, T., Yu, Z.C., Singarayer, J.S., Zürcher, S., Lettenmaier, D.P., Beerling, D.J., Denisov, S.N., Prigent, C., Papa, F., and Kaplan, J.O. (2013) Present state of global wetland extent and wetland methane modelling: methodology of a model inter-comparison project (WETCHIMP). *Geoscientific Model Development* 6:617–641.

Webster, C.R., Mahaffy, P.R., Atreya, S.K., Flesch, G.J., Mischna, M.A., Meslin, P.-Y., Farley, K.A., Conrad, P.G., Christensen, L.E., Pavlov, A.A., Martín-Torres, J., Zorzano, M.-P., McConnochie, T.H., Owen, T., Eigenbrode, J.L., Glavin, D.P., Steele, A., Malespin, C.A., Archer, P.D., Sutter, B., Coll, P., Freissinet, C., McKay, C.P., Moores, J.E., Schwenzer, S.P., Bridges, J.C., Navarro-González, R., Gellert, R., Lemmon, M.T., and the MSL Science Team. (2015) Mars methane detection and variability at Gale Crater. *Science* 347:415–417.

Weiss, B.P., Yung, Y.L., and Nealson, K.H. (2000) Atmospheric energy for subsurface life on Mars? *Proc Natl Acad Sci USA* 97:1395–1399.

Whalen, S. (2005) Biogeochemistry of methane exchange between natural wetlands and the atmosphere. *Environ Eng Sci* 22:73–94.

Yung, Y.L., Russell, M.J., and Parkinson, C.D. (2010) The search for life on Mars. *Journal of Cosmology* 5:1121–1130.

Yvon-Durocher, G., Allen, A.P., Bastviken, D., Conrad, R., Gudasz, C., St-Pierre, A., Thanh-Duc, N., and Del Giorgio, P.A. (2014) Methane fluxes show consistent temperature dependence across microbial to ecosystem scales. *Nature* 507:488–491.

Zahnle, K., Freedman, R.S., and Catling, D.C. (2011) Is there methane on Mars? *Icarus* 212:493–503.

Zent, A.P. and Quinn, R.C. (1995) Simultaneous adsorption of CO_2 and H_2O under Mars-like conditions and application to the evolution of the martian climate. *J Geophys Res: Planets* 100:5341–5349.

Zent, A.P. and Quinn, R.C. (1997) Measurement of H_2O adsorption under Mars-like conditions: effects of adsorbent heterogeneity. *J Geophys Res: Planets* 102:9085–9095.

Zent, A.P., Haberle, R.M., Houben, H.C., and Jakosky, B.M. (1993) A coupled subsurface-boundary layer model of water on Mars. *J Geophys Res: Planets* 98:3319–3337.

Zhang, S.Y., Talu, O., and Hayhurst, D.T. (1991) High-pressure adsorption of methane in zeolites Nax, Mgx, Cax, Srx and Bax. *J Phys Chem* 95:1722–1726.

Address correspondence to:
Renyu Hu
Jet Propulsion Laboratory
California Institute of Technology
Pasadena, CA 91109

E-mail: renyu.hu@jpl.nasa.gov

Abbreviations Used

DRH = deliquescence relative humidity
FTT = Fischer-Tropsch-type
MSL = Mars Science Laboratory
REMS = Rover Environmental Monitoring Station
SAM = Sample Analysis at Mars
TLS = Tunable Laser Spectrometer